Receptor editing in peripheral B cell tolerance

Jeffrey S. Rice*†, Jeffrey Newman*†, Chuansheng Wang*, Daniel J. Michael*, and Betty Diamond*‡§

Departments of *Microbiology and Immunology and ‡Medicine, Albert Einstein College of Medicine, Bronx, NY 10461

Receptor editing or secondary Ig gene rearrangement occurs in immature, autoreactive B cells to maintain self-tolerance. Here we show that nonspontaneously autoimmune mice immunized with a peptide mimetope of DNA develop peptide- and DNA-reactive antibodies. Antigen-specific B cells display a follicular B cell phenotype. As these cells move into the memory compartment, many express RAG protein and acquire expression of both κ and λ light chains. Thus, this study provides evidence for receptor editing occurring in a mature, antigen-activated B cell population. Because the receptor editing observed here occurred in an autoreactive response to antigen, it may function to maintain peripheral tolerance.

autoimmunity | B cell selection | autoantibodies

Autoreactive B cells routinely arise during the immune response to foreign antigen. Although it has been demonstrated that the processes of apoptosis, anergy, and receptor editing maintain tolerance in immature B cells, it is clear that autoreactivity can also arise in mature B cells in a germinal center response (1–4). Mechanisms that limit autoreactivity in this population are less well characterized. Studies investigating tolerance induction of antigen-specific B cells within a native repertoire have been limited by the rarity the population. In murine models of lupus, DNA-reactive B cells represent <0.1% of the splenic cell population (5). Thus, studies examining the fate of antigen-specific B cells have relied on transgenic mouse models, in which B cells expressing particular B cell receptors dominate the repertoire. Although analyses of these mice have been very informative, it is clear that the behavior of a B cell may differ when it competes for a particular niche within a lymphoid organ with other B cells (6–11). Thus, it remains important to study antigen-specific B cells within a complete B cell repertoire.

We have reported a peptide sequence (DWEYS-peptide) that behaves as a dsDNA mimetope (12). Immunization of nonspontaneously autoimmune BALB/c mice with an octameric form of this peptide (DWEYS-MAP) results in T cell-dependent production of pathogenic IgG anti-dsDNA antibodies (13, 14). To identify the dsDNA-reactive B cells participating in this response, we developed a specific staining methodology using a fluorochrome-labeled tetrameric form of the DWEYS peptide (DWEYS-tetramer) (15). We can use this technique to examine the development of a small autoreactive B cell population in the context of a normal repertoire.

We now demonstrate that dsDNA-reactive B cells arise in the follicular B cell population with little contribution from B1 or marginal zone B cells. As the autoreactive B cells mature, they undergo heavy chain class switching and develop phenotypic features of memory B cells. Furthermore, they express RAG and many acquire coexpression of κ and λ light chains. Thus, the activation of anti-dsDNA B cells is accompanied by light chain receptor editing. This may be a mechanism for maintaining tolerance in the periphery.

Experimental Procedures

Tetramer Generation. DWEYSVWLSN-streptavidin-allophycocyanin (DWEYS-APC) tetramers, DWEYSVWLSN-streptavidin-Alexa Fluor488 (DWEYS-A488) tetramers, and ADGSGGRDEMQASMWS-streptavidin-APC (10-2-APC) tetramers were generated as described (15). Biotinylated peptide was synthesized by AnaSpec (San Jose, CA). Fluorescent streptavidin was purchased from Molecular Probes. Inhibitor used unlabeled streptavidin.

Mice and Immunizations. Six- to 8-week-old female BALB/c and BALB/c SCID mice (The Jackson Laboratory) were housed in accord with American Association of Laboratory Animal Care regulations. BALB/c × RAG2:GFP mice were generated by crossing BALB/c mice with RAG2:GFP mice on a C57BL/6 × 129 background (generously donated by D. Nemazee, Scripps Research Institute, La Jolla, CA). Mice were immunized i.p. on day 0 with 100 μl of a 1:1 emulsion of complete Freund's adjuvant (Difco) containing 100 μg of DWEYSVWLSN peptide on a branched polylysine backbone (DWEYS-MAP, AnaSpec), or 100 μg of 10-2 peptide on a BSA carrier. On day 7, mice were boosted with 100 μg of DWEYS-MAP in incomplete Freund's adjuvant (Difco).

For further details, see *Supporting Text*, which is published as supporting information on the PNAS web site.

Flow Cytometry. Spleens were harvested from immunized mice. Bone marrow was harvested from tibias and femurs. Erythrocytes were lysed, and cell suspensions were stained in Hanks' balanced salt solution (Invitrogen/Gibco) with 0.3% FCS, pH 7.4. Inhibitor was added to cell suspensions before staining at 10-fold molar excess. The following antibodies were used: phycoerythrin (PE)-anti-CD24 (HSA, clone M1/69, Pharmingen), APC-anti-CD45R (B220, clone RA3–6B2, Pharmingen), PE-anti-C1qRp (AA4.1, eBioscience), FITC-anti-GL7 (GL7, Pharmingen), FITC-anti-IgD (11–26c.2a, Pharmingen), PE-anti-IgM (R6–60.2, Pharmingen), PE-anti-λ (goat polyclonal, Southern Biotechnology Associates), FITC-anti-κ (X36, Pharmingen), anti-active caspase-3 (CPP32, rabbit polyclonal, Pharmingen), and FITC-anti-rabbit-γ (goat polyclonal, Southern Biotechnology Associates).

Data were acquired by using a FACSCalibur flow cytometer and CELLQUEST software (Becton Dickinson Immunocytometry Systems). Analysis was performed by using FLOJO software (TreeStar, San Carlos, CA). Bivariate plots are presented as 5% probability contours. For futher details, see *Supporting Text*.

Cell Sorting. For sorting of the tetramer populations, splenocytes from five mice were pooled and isolated as described above. Cells were incubated with 50 μl each of biotinylated anti-CD3e (clone 145–2C11, Pharmingen), anti-CD11b (M1/70, Pharmingen), and anti-CD11c (HL3, Pharmingen) for 30 min at 4°C. Cells were washed, incubated with 100 μl per 4 × 10^7 cells streptavidin Dynabeads (Dynabeads M-280, Dynal, Brown Deer, WI) for 30 min at 4°C, and depleted of T cells, macrophages, monocytes, and dendritic cells on a Dynal MPC-1 magnet. Staining was performed as described above. Immediately after sorting, cells were resuspended in Trizol (Invitrogen) and frozen at −140°C until RNA isolation.
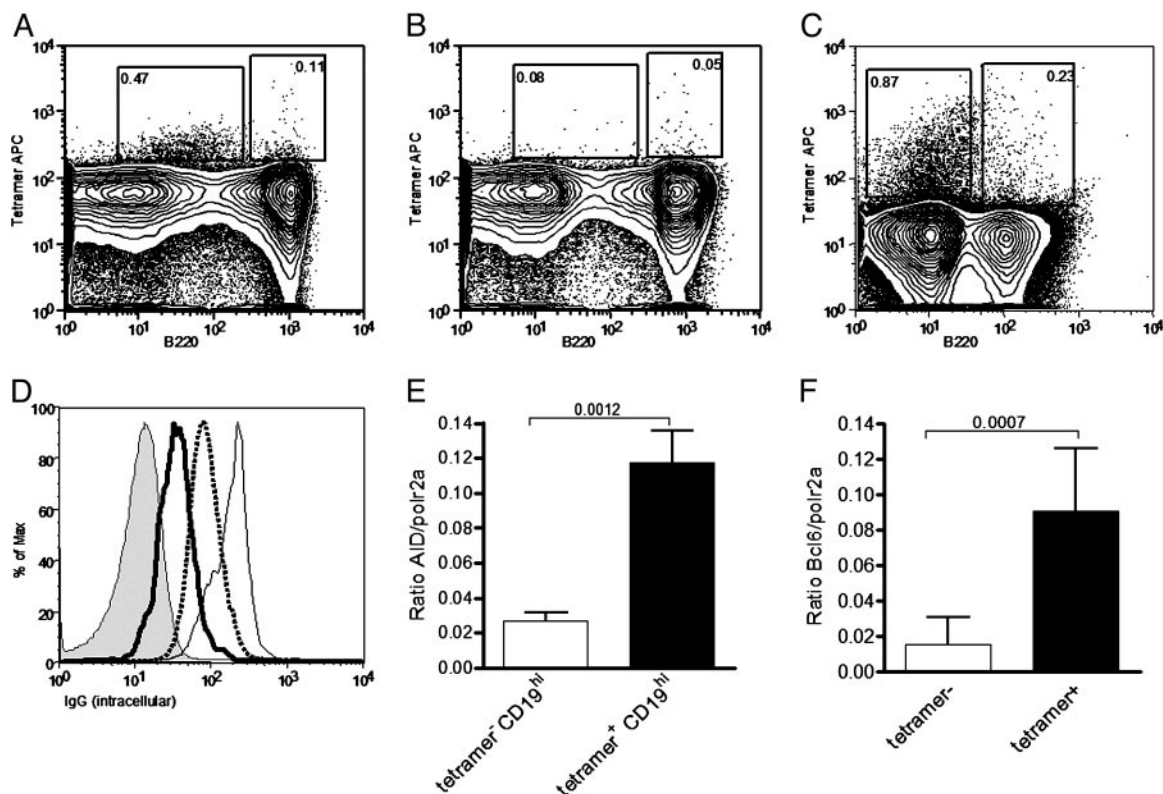

Fig. 1. Differentiation and maturity of tetramer-reactive splenocytes. (*A–C*) Representative tetramer staining after secondary challenge in the spleen (*A*) and inhibition of splenic staining by 30 mM nonfluorescent tetramer (*B*) and bone marrow (*C*). (*D*) Histogram of intracellular IgG staining in tetramer populations. Thick line, tetramer$^+$B220^{low}; thin line, tetramer$^+$B220^{hi}; dotted line, tetramer$^-$B220^{hi}; shaded line, tetramer$^-$B220$^-$. (*E*) Expression of AID in tetramer populations as determined by real-time PCR. (*F*) Expression of Bcl-6 in tetramer populations as determined by real-time PCR. Data in *A–D* are representative of 10 mice. Real-time PCR in *E* and *F* is representative of three independent experiments.

Sorting was performed on a MoFlo (DakoCytomation, Fort Collins, CO).

Histology. Spleens were removed on day 15 and frozen in Tissue-Tek OCT Compound (Miles, Elkhart, IN). Staining was performed in 3% FCS + 0.2% Triton X-100 for 30 min at room temperature. Tetramer staining was performed at 4°C overnight. Slides were mounted in Aqua-Poly/Mount (Polysciences, Inc, Warrington, PA). Fluorescent microscopy was performed on an AxioCam II (Carl Zeiss Microimaging, Thornwood, NY) with Axiovision 3.1. The following antibodies were used: Alexa Fluor488-anti-GFP (rabbit polyclonal, Molecular Probes), biotin-anti-CD11b (clone M1/70, Pharmingen), PE-anti-B220 (RA3–6B2, Pharmingen), anti-RAG1 (G109–256, Pharmingen), anti-RAG2 (rabbit polyclonal, Pharmingen), streptavidin-AMCA (Vector Laboratories). Anti-RAG antibodies were labeled by using Zenon Alexa Fluor 350 anti-mouse IgG2b or anti-rabbit IgG, and Alexa Fluor 488 anti-rabbit IgG (Molecular Probes).

Adoptive Transfers. For RAG2:GFP$^{+/-}$ transfers (see Fig. 3*E*), spleens were removed from naive donor mice and lymphocytes isolated as described above. Mice received 4×10^7 cells each by retro-orbital injection. Two weeks after transfer, recipient mice were immunized according to the protocol described. For further details, see *Supporting Text*.

Real-Time PCR. RNA was isolated from sorted cells by using TriZol reagent (Invitrogen) following the manufacturer's recommendations. Random hexamer-primed RT-PCR was performed on 5 μl of RNA by using SuperScript II reverse tran-

scriptase (Invitrogen) in 100-μl final volume, according to the manufacturer's protocol. Real-time PCR was performed by using an ABI 7900 (Applied Biosystems) and analyzed by using SDS version 2.2. ABI Gene Expression Assays were used, and the reactions were performed by using TaqMan Universal PCR Master Mix in 10-μl final volume. Standard curves were made for each experiment by using total spleen and bone marrow cDNA. Relative template concentration was determined from the standard curve by using Cts determined by the SDS software. All primers used spanned an intron/exon border. ABI Primer Ids were: RAG2, Mm00501300_m1; AID, Mm0050774_m1; Bcl6, Mm00477633_m1; RNA pol2a, Mm00839493_m1.

Results

Phenotypic Analysis of the Tetramer-Reactive B Cells. After immunization with DWEYS-MAP, tetramer-reactive splenic B cells can be identified with fluorescently tagged antigen (15). Two populations are observed: one population with high B220 expression (B220^{hi}tetramer$^+$), and a second population, comprising the majority of tetramer-reactive cells, with low B220 expression (B220^{low}tetramer$^+$) (Fig. 1*A*). Extensive studies of tetramer-reactive cells demonstrate that tetramer binding occurs only in mice immunized with the DWEYS-peptide, and is inhibitable by unlabeled tetramer (Fig. 1*B*). We have previously confirmed their B cell lineage (15). Interestingly, the B220^{low}tetramer$^+$ population is expanded in the bone marrow (Fig. 1*C*). Intracellular expression of IgG was observed in both tetramer-reactive populations (Fig. 1*D*). GL7 was highly induced on the B220^{hi} population (Table 1, which is published as supporting information on the PNAS web site), and real-time PCR analysis detected AID expression in this population (Fig.
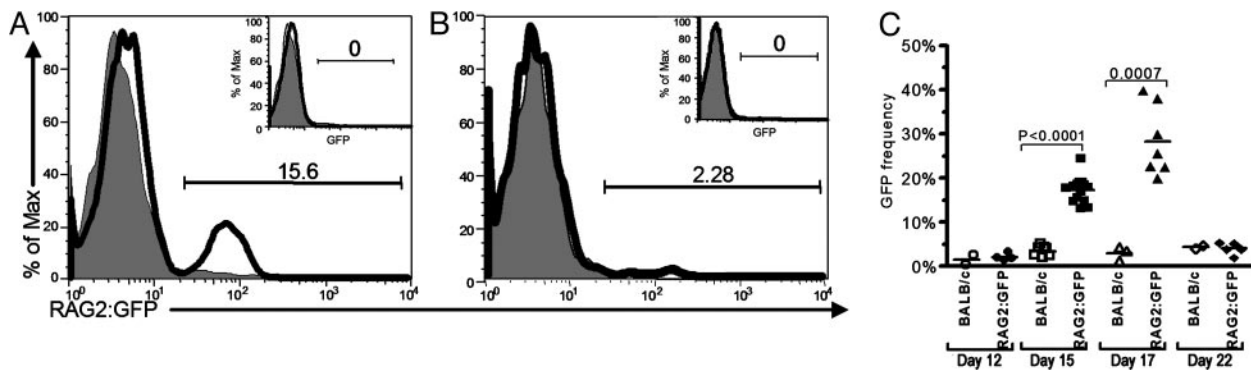
Fig. 2. RAG expression in tetramer-reactive B cells. (*A* and *B*) Representative histogram of GFP expression on day 15 in B220$^+$HSA^{low} DWEYS$^+$ (*A*) and 10-2$^+$ (*B*) B cells from RAG2:GFP Tg mice (solid line) compared to B220$^+$HSA^{low}tetramer$^+$ B cells in wild-type mice (shaded line). GFP expression is not seen in B220$^+$HSA^{low}tetramer$^-$ B cells in RAG2:GFP Tg mice (*Insets*). (*C*) Time course of GFP expression in DWEYS-immunized RAG2:GFP Tg mice versus wild-type mice.

1*E*). Finally, Bcl-6 was found to be expressed in both the B220^{hi} and B220^{low}tetramer$^+$ populations (Fig. 1*F*). These findings are consistent with a germinal center (16–19) and a memory B cell population (20). Additional phenotypic analysis (Table 1) supports this interpretation, and suggests that the B220^{hi} population contains precursors of the B220^{low} population.

RAG Expression Is Induced in Antigen-Binding B Cells. To determine whether there was any attempt to regulate the autoreactivity arising in response to DWEYS-MAP immunization, we looked for evidence of receptor editing in tetramer-reactive B cells. We used mice with a functional RAG2/GFP fusion gene inserted into the endogenous RAG2 locus (21) that allows for tracking of RAG2-expressing cells by their GFP fluorescence while maintaining the degradation sequences present on the wild-type protein and critical to ensuring a normal pattern of RAG expression. BALB/c × RAG2:GFP F1 mice were immunized twice with DWEYS-MAP or an irrelevant peptide, 10-2-BSA, and mature splenic B cells (B220^{hi} HSA^{low}) were analyzed for GFP expression. By day 15 after immunization, DWEYS-specific B cells expressed GFP (Fig. 2*A*), but the 10-2-specific population did not (Fig. 2*B*). No GFP expression was observed in mature B cells that were not activated by antigen (B220^{hi} HSA^{low}tetramer$^-$, Fig. 2 *A* and *B Insets*). Kinetic studies revealed that GFP expression arose >12 days after immunization, and declined by 22 days (Fig. 2*C*). Thus, GFP expression occurred only in mature B cells specific to the dsDNA mimetope, was absent in mature B cells specific to a non-self peptide (Fig. 3*A*), and displayed a kinetics consistent with antigen induction. To confirm RAG2 expression, splenocytes were transferred from RAG2:GFP mice into SCID recipients. Recipient mice were rested for 2 weeks to allow for engraftment. Because there is no emigration of new B cells from the bone marrow in SCID mice, the B cell population in the recipient mice consists exclusively of mature cells (22). Mice were immunized and GFP expression was observed in the tetramer$^+$ population, confirming that the expression of the RAG2:GFP fusion protein can occur in mature B cells (Fig. 3*B*).

Additional evidence for antigen-induced RAG2 expression was acquired by histological analysis of the spleen. GFP-positive cells were present primarily in the red pulp of DWEYS-MAP immunized mice (Fig. 4*C*) but not in naive (Fig. 4*A*) or 10-2-immunized (Fig. 4*B*) littermates. Staining of DWEYS-MAP immunized BALB/c mice with anti-RAG1 (Fig. 4*D*) and anti-RAG2 (Fig. 4*E*) antibodies demonstrated that both proteins were coexpressed in splenic B cells of DWEYS-MAP-

Fig. 4. Histological analysis of RAG2:GFP and BALB/c mice. (*A–C*) RAG2:GFP$^{+/-}$ spleen sections stained with anti-B220 (red), anti-CD11b (blue), and anti-GFP (green) in naive (*A*), 10-2-immunized (*B*), and DWEYS-immunized (*C*) mice. Images were obtained by using the ×10 objective. (*D–F*) BALB/c spleen sections from DWEYS-immunized mice stained with anti-RAG1 (*D*) or anti-RAG2 (*E*), and superimposed (*F*). Images were obtained by using the ×40 objective.

Fig. 3. RAG expression in autoreactive, mature B cells. (*A*) GFP expression in B220$^+$HSA^{low}tetramer$^+$ B cells from DWEYS (filled circles) and 10-2 (open circles) immunized RAG2:GFP Tg mice. (*B*) GFP expression in B220$^+$HSA^{low}tetramer$^+$ B cells after adoptive transfer and challenge.

Fig. 5. Histological staining with fluorescent tetramers. (*A* and *B*) BALB/c spleen sections from 10-2 (*A*) or DWEYS (*B*) immunized mice stained with anti-B220 (red) and DWEYS-A488 (green). Images were obtained by using the ×10 objective. (*C–F*) BALB/c spleen sections from DWEYS immunized mice stained with anti-B220 (*C*, red), DWEYS-A488 (*D*, green), anti-RAG2 (*E*, blue), and superimposed (*F*). Images were obtained by using the ×40 objective.

Fig. 6. Real-time PCR analysis of RAG2 expression and analysis of receptor editing. (*A*) Real-time PCR analysis of RAG2 expression versus RNA polymerase 2 (housekeeping gene) in mature B cells (B220$^+$HSA^{low}AA4.1^{low}) from naive, DWEYS-, or 10-2-immunized mice. (*B*) Ratio of RAG2 expression in mature versus immature (B220$^+$HSA^{hi}AA4.1^{hi}) B cells in naive, DWEYS-, or 10-2-immunized mice.

immunized mice (Fig. 4*F*), but not in naive or 10-2-immunized BALB/c or RAG2:GFP$^{+/-}$ mice (data not shown).

Staining by the DWEYS tetramer was observed again in the red pulp of BALB/c mice immunized with DWEYS-MAP (Fig. 5*A*) and not in mice immunized with 10-2 (Fig. 5*B*) or in naive littermates (data not shown). Some DWEYS-reactive B cells were present in B cell follicles; these cells were IgM$^+$ (data not shown). Costaining with anti-B220 (Fig. 5*C*), DWEYS-tetramer (Fig. 5*D*), and anti-RAG2 (Fig. 5*E*) revealed that RAG2 expression was limited to DWEYS-reactive B220$^+$ cells (Fig. 5*F*). Consistent with the flow cytometry data, no RAG expression was observed in cells not binding to the tetramer.

Real-Time PCR Analysis of RAG2 Expression. To confirm RAG2 expression, mature B cells (B220$^+$AA4.1^{low}HSA^{low}) were isolated from DWEYS-MAP or 10-2-BSA immunized and naive BALB/c mice. Real-time PCR for RAG2 revealed expression of RAG2 RNA only in splenocytes isolated from DWEYS-MAP immunized mice (Fig. 6*A*), and was specific to mature B cells (Fig. 6*B*).

Receptor Editing in Tetramer-Reactive Cells. Receptor editing leaves characteristic molecular signatures, one of which is coexpression of κ and λ light chains (23). Therefore, we investigated the pattern of light chain expression on tetramer-reactive B cells. Fig. 7*A* shows that a majority (81.3%) of the tetramer-reactive cells coexpressed κ and λ light chains. λ light chain coexpression was related to antigen-induced differentiation because <5% of nontetramer binding B cells (B220^{hi}tetramer$^-$) coexpressed κ and λ light chains, and B220^{hi}tetramer$^+$ cells still expressing IgD showed a lower incidence of λ expression than those that had undergone heavy chain class switching (data not shown).

If receptor editing is a mechanism to regulate autoreactivity,

there should be little editing in a nonautoreactive response. Therefore, we characterized B cells in mice immunized with 10-2-BSA (24) for coexpression of two surface light chains to see whether this was related to autoreactivity. Consistent with the absence of RAG in responding B cells, the κ and λ positive population was not observed (Fig. 7*B*).

To demonstrate that expression of λ light chains follows antigen activation, splenocytes from BALB/c mice were transferred to SCID mice. The donor cells were allowed 14 days to colonize the SCID recipients, during which time any immature B cells that have been transferred either mature or die (22). The recipients were then immunized with DWEYS-MAP. Early in the response, no antigen-specific cells were positive for both κ and λ light chain expression (data not shown). By day 15 after immunization, a significant number (57%) of tetramer-reactive B cells displayed both κ and λ light chains (Fig. 7*C*).

Receptor editing is a mechanism to generate nonautoreactive specificities. If receptor editing fails to produce a nonautoreactive receptor, autoreactive B cells may continue along an apoptotic pathway. Therefore, we looked to see whether mature tetramer$^+$ cells also showed evidence of deletion that might result from failed secondary rearrangement (Fig. 8*A*). λ rearrangement occurs secondary to κ rearrangement, and is common in B cells that have undergone receptor editing. Expression of activated caspase-3 was highest in antigen-specific cells that expressed λ, and may represent cells that have undergone editing but failed to eliminate autoreactivity.

To demonstrate that light chain surface expression by the tetramer-binding population is not the result of passive absorption of serum antibody, we isolated RNA from B220^{low}tetramer$^+$, B220^{hi}tetramer$^+$, and B220^{hi}tetramer$^-$ cells and performed RT-PCR for λ and β-actin mRNA. A 3.6-fold increase in the ratio of the λ signal to the β-actin signal was noted in the B220^{low}tetramer$^+$ population relative to the B220^{hi}tetramer$^+$ and the overall B220^{hi} populations (Fig. 8*B*). Thus, the synthesis of λ light chain mRNA by the B220^{low}tetramer$^+$ population was confirmed.

Discussion

Taking advantage of a peptide mimetope for dsDNA identified in our laboratory, biotinyl-peptides were bound to streptavidin–fluorochrome molecules, creating avidity-enhanced fluorescent tetramers. We have demonstrated that the tetramers can identify the small number of peptide- and dsDNA-reactive B cells that are present within the B cell repertoire of a mouse (15). We have tracked the development of these cells, showing that they mature as follicular B cells. Mechanisms of negative selection operate on these autoreactive B cells and receptor editing occurs after antigen activation to eliminate autoreactive B cells.

After immunization with the peptide mimetope for DNA, two tetramer-reactive populations were identified in BALB/c mice,

Fig. 7. Analysis of light chain expression. (*A*) Bivariate plots depicting λ and κ staining of DWEYS tetramer-gated cells. (*B*) Bivariate plots depicting κ and λ staining of 10-2 tetramer-gated cells. (*C*) Bivariate plots depicting λ and κ staining of DWEYS tetramer gated cells from SCID recipients of BALB/c splenocytes.

one that was B220^{hi} and the other B220^{low}. The B220^{hi}tetramer$^+$ population demonstrated high levels of costimulatory molecules, consistent with recent activation, whereas the B220^{low}tetramer$^+$ population expressed lower levels of these markers. B220^{hi}tetramer$^+$ cells also express germinal center markers. Phenotypic characteristics of the populations suggest movement from the B220^{hi} to the B220^{low} compartment. Although it has been suggested that the B220^{low} antigen-specific cells can result from antibody bound by Fc receptors on non-B cells (25), we present evidence that the antigen-specific cells in our model are B cells (Figs. 9 and 10, which are published as supporting information on the PNAS web site). We show a lack of tetramer staining B cells despite high serum antibody titers in naive mice given immune serum, and tetramer staining B cells despite a lack of serum antibody titers in naive mice given immune B cells by adoptive transfer.

The B220^{low}tetramer$^+$ population possesses many characteristics of a memory B cell population. McHeyzer-Williams and colleagues (26, 27) reported a B220^{low} memory population in NP-immunized mice. A B220^{low} memory population has been observed also in the quasimonoclonal mouse (28), and human memory B cells have been shown to down-regulate B220 expression (29, 30). Furthermore, it has been suggested that Bcl-6, which is expressed in the B220^{low} population, is involved in memory B cell maintenance (20). The data in Table 1 further suggest that the B220^{low}tetramer$^+$ population contains two subsets of B cells: one that differentiates into plasma cells, and one that becomes memory cells. In accordance with this, a subset of the B220^{low}tetramer$^+$ cells express CD138 (data not shown) and is present in the bone marrow.

Fig. 8. Expression of activated caspase-3 and λ light chain. (*A*) Active caspase-3 expression in B220$^+$ (circles), DWEYS$^+$λ$^-$ (squares), and DWEYS$^+$λ$^+$ B cells (triangles). (*B*) Densitometric quantitation of λ light chain/actin RNA as determined by semiquantitative RT-PCR on the indicated sorted populations.

Secondary rearrangement of antibody genes in immature B cells in the bone marrow is well established. Evidence for secondary rearrangements in mature B cells has been controversial. Studies of murine germinal center B cells have shown expression of RAG protein by immunohistology (31) and RAG mRNA by RT-PCR and Southern blotting (32, 33). Activation of splenic B cells by IL-4 and LPS or CD40L has also been shown to induce RAG expression (33). Studies of healthy human subjects have found evidence of RAG expression in germinal center centrocytes and memory B cells (23, 34, 35). RAG expression has also been found in B cells in the synovial tissue of rheumatoid arthritis patients and in the peripheral blood B cells of SLE patients (36, 37).

Recently, three lines of RAG-indicator mice have been developed (21, 38, 39). Each line permits monitoring of RAG expression (either RAG1 or RAG2) by linking RAG expression to GFP expression. In each of the GFP-RAG indicator models, the authors identify peripheral B cells expressing RAG, but conclusive assignment to the mature compartment was not possible. The failure to demonstrate a mature population of B cells undergoing receptor editing is likely to be a reflection of the rarity of such cells. In the study by Monroe *et al.* (21), GFP expressing antigen-specific B cells with markers of germinal center cells were seen when an antigen-specific population was analyzed. Although it was postulated that these may be immature B cells recruited to the germinal center response, the data were also consistent with reexpression of RAG genes in mature B cells.

To confirm in our study that receptor editing was occurring selectively in B cells responding to antigen, we immunized RAG2:GFP × BALB/c F$_1$ mice with DWEYS-MAP. These mice express a GFP-RAG2 fusion protein under the direction of the RAG2 promoter, as described by Monroe *et al.* (21). Mature tetramer-binding B cells expressed GFP, whereas the mature B cells that did not respond to peptide showed no expression of GFP. Thus, RAG expression is linked to antigen activation. GFP expression was present for a short time after antigenic challenge in a model of induced autoreactivity, but not in a nonautoreactive response, suggesting that receptor editing is a mechanism to generate peripheral tolerance and that there is a limited period during which mature antigen-activated B cells can undergo this process. Moreover, the response to the dsDNA mimetope and the induction of RAG correlated with the coexpression of κ and λ by tetramer-binding cells. We confirmed by adoptive transfer that RAG expression occurred in mature cells in this system. We speculate that B cells leaving the germinal center can, like transitional B cells, be induced to undergo receptor editing and

apoptosis if they encounter soluble antigen. This might account for the occurrence of receptor editing in autoreactive, but not nonautoreactive, cells.

In summary, the data presented here demonstrate the importance of studying the emergence of autoreactivity in wild-type animals in an antigen-specific manner. The ability to examine rare populations of cells that have a particular antigenic specificity will allow us to probe B cell regulation to a degree not previously possible. We can now recognize that as follicular B cells differentiate in an antigen-induced response, negative selection of autoreactive cells occurs concomitant with the transition to the memory or plasma cell compartment. Because our initial observation that somatic mutation can lead to the generation of autospecificity in B cells (1), we and others have shown that autoreactive B cells are generated at high frequency during the response to certain antigens (2, 3). Previous studies have also demonstrated that despite the activation of autoreac-

tive B cells in a primary response to antigen, there is an absence of these cells in the memory B cell population (40, 41). The methodology used in the current study reveals that receptor editing is responsible for the elimination of autoreactivity that occurs in antigen-activated B cells. RAG expression and editing may lead to translocations of the Ig locus that contribute to B cell malignancy in germinal center cells, and may explain why such tumors are often autoreactive.

This study demonstrates that the processes that govern negative selection after diversification of the repertoire in naive B cells may also operate in the antigen activated B cell repertoire. The ability of mature B cells to undergo secondary Ig rearrangement confirms that the mechanisms important in the maintenance of tolerance in immature B cells also function in the mature population.

1. Diamond, B. & Scharff, M. D. (1984) *Proc. Natl. Acad. Sci. USA* **81,** 5841–5844.
2. Benschop, R. J., Aviszus, K., Zhang, X., Manser, T., Cambier, J. C. & Wysocki, L. J. (2001) *Immunity* **14,** 33–43.
3. Ray, S. K., Putterman, C. & Diamond, B. (1996) *Proc. Natl. Acad. Sci. USA* **93,** 2019–2024.
4. Hande, S., Notidis, E. & Manser, T. (1998) *Immunity* **8,** 189–198.
5. Klinman, D. M., Shirai, A., Ishigatsubo, Y., Conover, J. & Steinberg, A. D. (1991) *Arthritis Rheum.* **34,** 1404–1410.
6. Cyster, J. G., Hartley, S. B. & Goodnow, C. C. (1994) *Nature* **371,** 389–395.
7. Cyster, J. G. & Goodnow, C. C. (1995) *Immunity* **3,** 691–701.
8. Mandik-Nayak, L., Bui, A., Noorchashm, H., Eaton, A. & Erikson, J. (1997) *J. Exp. Med.* **186,** 1257–1267.
9. Mandik-Nayak, L., Seo, S. J., Sokol, C., Potts, K. M., Bui, A. & Erikson, J. (1999) *J. Exp. Med.* **189,** 1799–1814.
10. Dal Porto, J. M., Haberman, A. M., Kelsoe, G. & Shlomchik, M. J. (2002) *J. Exp. Med.* **195,** 1215–1221.
11. Lesley, R., Xu, Y., Kalled, S. L., Hess, D. M., Schwab, S. R., Shu, H. B. & Cyster, J. G. (2004) *Immunity* **20,** 441–453.
12. Gaynor, B., Putterman, C., Valadon, P., Spatz, L., Scharff, M. D. & Diamond, B. (1997) *Proc. Natl. Acad. Sci. USA* **94,** 1955–1960.
13. Putterman, C. & Diamond, B. (1998) *J. Exp. Med.* **188,** 29–38.
14. Khalil, M., Inaba, K., Steinman, R., Ravetch, J. & Diamond, B. (2001) *J. Immunol.* **166,** 1667–1674.
15. Newman, J., Rice, J. S., Wang, C., Harris, S. L. & Diamond, B. (2003) *J. Immunol. Methods* **272,** 177–187.
16. Muramatsu, M., Sankaranand, V. S., Anant, S., Sugai, M., Kinoshita, K., Davidson, N. O. & Honjo, T. (1999) *J. Biol. Chem.* **274,** 18470–18476.
17. Onizuka, T., Moriyama, M., Yamochi, T., Kuroda, T., Kazama, A., Kanazawa, N., Sato, K., Kato, T., Ota, H. & Mori, S. (1995) *Blood* **86,** 28–37.
18. Niu, H., Cattoretti, G. & Dalla-Favera, R. (2003) *J. Exp. Med.* **198,** 211–221.
19. Cattoretti, G., Chang, C. C., Cechova, K., Zhang, J., Ye, B. H., Falini, B., Louie, D. C., Offit, K., Chaganti, R. S. & Dalla-Favera, R. (1995) *Blood* **86,** 45–53.
20. Fearon, D. T., Manders, P. & Wagner, S. D. (2001) *Science* **293,** 248–250.
21. Monroe, R. J., Seidl, K. J., Gaertner, F., Han, S., Chen, F., Sekiguchi, J., Wang, J., Ferrini, R., Davidson, L., Kelsoe, G. & Alt, F. W. (1999) *Immunity* **11,** 201–212.
22. Allman, D. M., Ferguson, S. E., Lentz, V. M. & Cancro, M. P. (1993) *J. Immunol.* **151,** 4431–4444.
23. Meffre, E., Papavasiliou, F., Cohen, P., de Bouteiller, O., Bell, D., Karasuyama, H., Schiff, C., Banchereau, J., Liu, Y. J. & Nussenzweig, M. C. (1998) *J. Exp. Med.* **188,** 765–772.
24. Harris, S. L., Dagtas, A. S. & Diamond, B. (2002) *Mol. Immunol.* **39,** 263–272.
25. Bell, J. & Gray, D. (2003) *J. Exp. Med.* **197,** 1233–1244.
26. McHeyzer-Williams, L. J., Cool, M. & McHeyzer-Williams, M. G. (2000) *J. Exp. Med.* **191,** 1149–1166.
27. Driver, D. J., McHeyzer-Williams, L. J., Cool, M., Stetson, D. B. & McHeyzer-Williams, M. G. (2001) *J. Immunol.* **167,** 1393–1405.
28. Cascalho, M., Wong, J., Brown, J., Jack, H. M., Steinberg, C. & Walb, M. (2000) *Int. Immunol.* **12,** 29–35.
29. Bleesing, J. J. H., Morrow, M. R., Uzel, G. & Fleisher, T. A. (2001) *Cell. Immunol.* **213,** 72–81.
30. Bleesing, J. J. H. & Fleisher, T. A. (2003) *Cytometry B* **51,** 1–8.
31. Han, S., Zheng, B., Schatz, D. G., Spanopoulou, E. & Kelsoe, G. (1996) *Science* **274,** 2094–2097.
32. Hikida, M., Mori, M., Kawabata, T., Takai, T. & Ohmori, H. (1997) *J. Immunol.* **158,** 2509–2512.
33. Hikida, M., Mori, M., Takai, T., Tomochika, K., Hamatani, K. & Ohmori, H. (1996) *Science* **274,** 2092–2094.
34. Giachino, C., Padovan, E. & Lanzavecchia, A. (1998) *Eur. J. Immunol.* **28,** 3506–3513.
35. Girschick, H. J., Grammer, A. C., Nanki, T., Mayo, M. & Lipsky, P. E. (2001) *J. Immunol.* **166,** 377–386.
36. Itoh, K., Meffre, E., Albesiano, E., Farber, A., Dines, D., Stein, P., Asnis, S. E., Furie, R. A., Jain, R. I. & Chiorazzi, N. (2000) *J. Exp. Med.* **192,** 1151–1164.
37. Girschick, H. J., Grammer, A. C., Nanki, T., Vazquez, E. & Lipsky, P. E. (2002) *Arthritis Rheum.* **46,** 1255–1263.
38. Kuwata, N., Igarashi, H., Ohmura, T., Aizawa, S. & Sakaguchi, N. (1999) *J. Immunol.* **163,** 6355–6359.
39. Yu, W., Nagaoka, H., Jankovic, M., Misulovin, Z., Suh, H., Rolink, A., Melchers, F., Meffre, E. & Nussenzweig, M. C. (1999) *Nature* **400,** 682–687.
40. Notidis, E., Heltemes, L. & Manser, T. (2002) *Immunity* **17,** 317–327.
41. Kuo, P., Bynoe, M. & Diamond, B. (1999) *Mol. Immunol.* **36,** 471–479.

IMMUNOLOGY